Journal of Sound and Vibration (1997) **206**(4), 589–604

STABILITY AND BIFURCATIONS OF LIMIT CYCLES BY THE PERTURBATION–INCREMENTAL METHOD

H. S. Y. Chan and K. W. Chung

Department of Mathematics, City University of Hong Kong, Hong Kong

and

Z. Xu

Department of Mechanics, Zhongshan University, Guangzhou, People's Republic of China

(*Received* 6 *September* 1995, *and in final form* 24 *May* 1997)

The perturbation–incremental method is applied to the study of stability bifurcations of limit cycles and homoclinic (heteroclinic) bifurcations of strongly non-linear oscillators. The bifurcation parameters can be determined to any desired degree of accuracy.

1. INTRODUCTION

Consider practical systems governed by the equation

$$\ddot{x} + g(x) = \lambda f(x, \dot{x}, \mu)\dot{x}, \tag{1}$$

where g and f are arbitrary non-linear functions of their arguments, and λ and μ are parameters of arbitrary magnitude. It will be assumed that equation (1) possesses at least one limit cycle solution enclosing the origin of the $x - \dot{x}$ phase plane. The problem of determining the variations of limit cycles for equation (1) as the parameters λ and μ change is of special interest.

For small λ, Holmes and Rand [1] have studied the case when $g(x)$ is linear plus cubic polynomial terms by using the methods of differentiable dynamics. Coppola and Rand [2], Margallo and Bejarano [3] have also treated such problems using the Jacobian elliptic functions. The case for general non-linear function $g(x)$ and including forced response have been considered by Xu and co-workers in a number of publications [4–7] extending the classical perturbation techniques and average methods. The parameter λ is, however, still restricted to a low value by the perturbation requirements.

Recently, the authors presented a perturbation–iterative method [8] which can be applied to moderately large values of parameter λ. In case λ is arbitrary, another procedure called the perturbation–incremental method [9] was formulated and later extended in [10] to calculate also the separatrices of the oscillator. In this paper, the perturbation–incremental method is used to find the stability bifurcations of limit cycles. The number of limit cycles will also be determined. To the authors' knowledge, no practical numerical procedures exist in the literature for the determination of semi-stability of limit cycles. Homoclinic (heteroclinic) bifurcations will also be discussed as in [10]. The parameter values of bifurcations, portraits of limit cycles and homoclinic (heteroclinic) orbits can be calculated to any desired degree of accuracy.

0022–460X/97/390589 + 16 $25.00/0/sv971128

2. STABILITY BIFURCATIONS OF LIMIT CYCLES

Following references [8, 9], limit cycles can be represented in parametric form by assuming

$$x = a\cos\varphi + b, \qquad \dot{x} = -a\Phi(\varphi)\sin\varphi, \tag{2}$$

where a is the amplitude, b the bias and φ is the new time with

$$\mathrm{d}\varphi/\mathrm{d}t = \Phi(\varphi), \qquad \Phi(\varphi + 2\pi) = \Phi(\varphi) > 0.$$

In the φ domain, equation (1) can be integrated once to give

$$\tfrac{1}{2}(\Phi\sin\varphi)^2 + \tilde{v}(a, b, \varphi) - \lambda\int_0^{\varphi}\tilde{f}(a, b, \mu, \Phi, \theta)\mathrm{d}\theta = 0, \tag{3}$$

where

$$v(x) = \int_0^x g(u)\mathrm{d}u, \qquad \tilde{v}(a, b, \varphi) = \frac{[v(a\cos\varphi + b) - v(a + b)]}{a^2},$$

$$\tilde{f}(a, b, \mu, \Phi, \theta) = f(a\cos\theta + b, -a\Phi\sin\theta, \mu)\Phi\sin^2\theta,$$

and from the regularization conditions

$$\tilde{v}(a, b, \pi) - \lambda\int_0^{\pi}\tilde{f}(a, b, \mu, \Phi, \theta)\,\mathrm{d}\theta = 0, \tag{4}$$

$$\int_0^{2\pi}\tilde{f}(a, b, \mu, \Phi, \theta)\,\mathrm{d}\theta = 0. \tag{5}$$

The characteristic exponent of the limit cycle is $\gamma = \lambda\tilde{\gamma}/T$, (see reference [9]) where

$$\tilde{\gamma} = \int_0^{2\pi}[f(a\cos\varphi + b, -a\Phi\sin\varphi, \mu) - a\Phi\sin f'_{\dot{x}}(a\cos\varphi + b, -a\Phi\sin\varphi, \mu)]\frac{\mathrm{d}\varphi}{\Phi(\varphi)}, \tag{6}$$

$$T = \int_0^{2\pi}\frac{\mathrm{d}\varphi}{\Phi(\varphi)}. \tag{7}$$

One will also write

$$f^*(a, b, \mu, \Phi, \varphi) = [f(a\cos\varphi + b, -a\Phi\sin\varphi, \mu) - a\Phi\sin\varphi f'_x(a\cos\varphi + b, -a\Phi\sin\varphi, \mu)]/\Phi(\varphi) \tag{8}$$

for convenience. The limit cycle is stable (unstable) if $\gamma < 0$ (>0). When the limit cycle is semistable at $\mu = \mu_0$, then $\gamma = 0$. A small change of the corresponding parameter value μ may cause the disappearance of the limit cycle or the occurrence of two limit cycles at this point. At $\mu = \mu_0$, there is one semi-stable limit cycle. There is no limit cycle on one side of μ_0, and there are two limit cycles on the other side of μ_0, one stable and one unstable. This kind of bifurcation is called the stability bifurcation of a limit cycle, (see for example

Zhang *et al*. [11]). The condition for semi-stable limit cycle is governed by the condition of zero characteristic exponent

$$\int_0^{2\pi} f^*(a, b, \mu, \Phi, \varphi)\, \mathrm{d}\varphi = 0, \tag{9}$$

and together with equations (3–5), the values at bifurcation can be determined. By applying the perturbation–incremental method to this problem, the procedure is divided into two steps (see reference [9]).

The first step is the perturbation method. Starting with a small value of $\lambda \approx 0$, the zero order perturbation solution for the semi-stable limit cycle of equation (1) is given by

$$x = a_0 \cos\varphi + b_0, \qquad \dot{x} = -a_0\, \Phi_0(\varphi) \sin\varphi,$$

where

$$\Phi_0(\varphi) = [2v(a_0 + b_0) - 2v(a_0 \cos\varphi + b_0)]^{1/2}/a_0\, |\sin\varphi|, \tag{10}$$

and the constants a_0, b_0 and μ_0 satisfy:

$$v(-a_0 + b_0) - v(a_0 + b_0) = 0, \qquad \int_0^{2\pi} \tilde{f}(a_0, b_0, \mu_0, \Phi_0, \varphi)\mathrm{d}\varphi = 0, \tag{11a, b}$$

$$\int_0^{2\pi} f^*(a_0, b_0, \mu_0, \Phi_0, \varphi)\mathrm{d}\varphi = 0. \tag{11c}$$

The second step of the perturbation–incremental is the parameter incremental method. Small increments are added to the current solution a_0, b_0, μ_0 and Φ_0 (or the perturbation solution at the beginning of the procedure) of equations (3–5) and (9), to obtain a neighbouring solution corresponding to $\lambda = \lambda_0 + \Delta\lambda$ and

$$a = a_0 + \Delta a, \qquad b = b_0 + \Delta b, \qquad \mu = \mu_0 + \Delta\mu, \qquad \Phi = \Phi_0 + \Delta\Phi. \tag{12}$$

Any 2π periodic function will have a Fourier expansion and one's basic assumption is that M harmonics will provide a sufficiently accurate representation. The exact number M is problem dependent; further discussion can be found in reference [10]. Therefore one writes

$$\Phi = \sum_{j=0}^{M} (P_j \cos j\varphi + Q_j \sin j\varphi), \qquad Q_0 = 0, \tag{13a}$$

$$\Delta\Phi = \sum_{j=0}^{M} (\Delta P_j \cos j\varphi + \Delta Q_j \sin j\varphi), \qquad \Delta Q_0 = 0. \tag{13b}$$

Expanding equations (3–5) and (9) by Taylor's series about the initial state and by applying the harmonic balance method to the linearized incremental equations, a system of linear equations is obtained with unknowns Δa, Δb, $\Delta\mu$, ΔP_j and ΔQ_j in the form

$$A_n\, \Delta a + B_n\, \Delta b + C_n\, \Delta\mu + A_{n,0}\, \Delta P_0 + \sum_{j=1}^{M} (A_{n,j}\, \Delta P_j + B_{n,j}\, \Delta Q_j) = R_n \tag{14}$$

for $n = 0, 1, 2, \ldots, 2M + 3$. R_n are residue terms. Derivation of the coefficients follows the same procedure as shown in references [9, 10].

Equations (14) are to be solved by an equation solver such as the Gaussian elimination procedure. The values a_0, b_0, μ_0 and Φ_0 are updated by adding together the original values and the corresponding incremental values. The iteration process continues until $R_n \to 0$ for all n, (in practice, $|R_n|$ is less than a desired degree of accuracy). The entire incremental process proceeds by adding $\Delta\lambda$ increment to the converged value of λ, using previous solution as initial approximation until a new converged solution is obtained.

For the stable limit cycle or unstable limit cycle, the characteristic exponent $\gamma \neq 0$. Therefore, equation (9) is not presented and should be eliminated from the system of equations (14). The total number of equations is one less than the total number of unknowns, and it is necessary to set either one of Δa, Δb or $\Delta\mu$ to zero for the solution of the other variables. In case μ is given, limit cycles are obtained by letting $\Delta\mu = 0$.

3. EXAMPLE OF STABILITY BIFURCATION

Consider the generalized Liénard oscillator of the form

$$\ddot{x} + x^3 = \lambda(1 - \mu x^2 + x^4)\dot{x}, \qquad \lambda > 0, \tag{15}$$

where $f(x, \dot{x}, \mu) = 1 - \mu x^2 + x^4$, $g(x) = x^3$. Hence $v(x) = x^4/4$. As

$$g(-x) = -g(x), \qquad f(-x, -\dot{x}, \mu) = f(x, \dot{x}, \mu), \tag{16}$$

Equation (15) is the same under the change of co-ordinates $x \to -x$, $\dot{x} \to -\dot{x}$. Therefore, the phase portrait will be symmetrical with respect to the origin. It follows that

$$x(\varphi + \pi) = -x(\varphi), \qquad \dot{x}(\varphi + \pi) = -\dot{x}(\varphi)$$

and by equation (2)

$$b = 0, \qquad \Phi(\varphi + \pi) = \Phi(\varphi). \tag{17}$$

Hence

$$\Phi(\varphi) = \sum_{j \geq 0} (P_{2j} \cos 2j\varphi + Q_{2j} \sin 2j\varphi). \tag{18}$$

3.1. THE ZERO ORDER PERTURBATION SOLUTION

From equations (10) and (11b), one has

$$\Phi_0(\varphi) = a_0 [\tfrac{1}{2}(1 + \cos^2 \varphi)]^{1/2} \tag{19}$$

and

$$\int_0^{2\pi} (1 - \mu a_0^2 \cos^2 \varphi + a_0^4 \cos^4 \varphi)\Phi_0(\varphi) \sin^2 \varphi \, \mathrm{d}\varphi = 0. \tag{20}$$

Equation (20) can be written as

$$\mu = \int_0^{2\pi} (1 + a_0^4 \cos^2 \varphi)\Phi_0(\varphi) \sin^2 \varphi \, \mathrm{d}\varphi \Big/ a_0^2 \int_0^{2\pi} \Phi_0(\varphi) \cos^2 \varphi \sin^2 \varphi \, \mathrm{d}\varphi$$

$$= [5\Gamma^2(\tfrac{1}{4})/84\Gamma^2(\tfrac{3}{4})]\,(7/a_0^2 + a_0^2) \overset{\text{def}}{=} \mu(a_0), \tag{21}$$

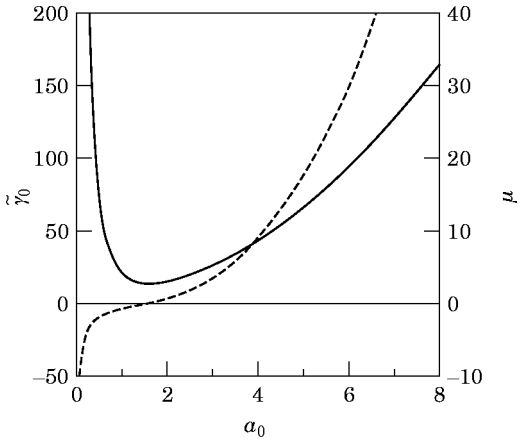

Figure 1. The parameter μ (——) and the characteristic exponent $\tilde{\gamma}_0$ (- - - -) versus amplitude a_0 of the limit cycle of equation (15) for the zero order perturbation solution.

where Γ is the gamma function. The characteristic exponent in equation (6) is now given by

$$\tilde{\gamma}_0 = \int_0^{2\pi} \frac{1 - \mu(a_0)a_0^2 \cos^2 \varphi + a_0^4 \cos^4 \varphi}{\Phi_0(\varphi)} \, \mathrm{d}\varphi = [2\sqrt{2\pi}\Gamma(\tfrac{1}{4})/21a_0 \, \Gamma(\tfrac{3}{4})] \, (a_0^4 - 7). \qquad (22)$$

The curves generated by using equations (21) and (22) are shown in Figure 1. Solutions exist for positive a_0 with a minimum value of $\mu = \mu_0^*$ attained for $a_0 = a_0^*$, where

$$a_0^* = (7)^{1/4} \simeq 1{\cdot}6266, \qquad \mu_0^* = [5\sqrt{7}\Gamma^2(\tfrac{1}{4})/42\Gamma^2(\tfrac{3}{4})] \simeq 2{\cdot}7573. \qquad (23)$$

a_0^* is also the value of a satisfying equation (11c), i.e., for which $\tilde{\gamma}_0 = 0$. Also, $\tilde{\gamma}_0 < 0$ for $a_0 < a_0^*$ and $\tilde{\gamma}_0 > 0$ for $a_0 > a_0^*$ as shown in Figure 1. The zero order approximation for the semi-stable limit cycle is then given by $x = (7)^{1/4} \cos \varphi$, $\dot{x} = -[3{\cdot}5(1+\cos^2 \varphi)]^{1/2} \sin \varphi$.

For small $\lambda > 0$, Figure 1 indicates that if $\mu < \mu_0^*$, equation (15) has no limit cycle; if $\mu > \mu_0^*$, equation (15) has two limit cycles with an unstable larger limit cycle and a stable smaller limit cycle.

3.2. THE PARAMETER INCREMENTAL SOLUTION

Results for larger values of λ are obtained by the incremental approach. $\lambda_0 = 0$ and $\Delta\lambda = 0{\cdot}5$ are assigned in equations (14). After 10 successive increments of $\Delta\lambda$ starting from the zero order solution (23), selected results are shown in Table 1 and plotted in a (λ, μ) diagram in Figure 2.

TABLE 1

Values of μ^* and a at the semi-stable limit cycles of equation (15) *for various λ*

λ	μ^*	a
~ 0	2·75730	1·62658
1·0	2·75862	1·62803
2·0	2·76344	1·63279
3·0	2·77339	1·64225
4·0	2·79227	1·65901
5·0	2·82146	1·68239

$\mu^* \simeq 2{\cdot}7573 + 0{\cdot}0012\lambda^{2{\cdot}413}$

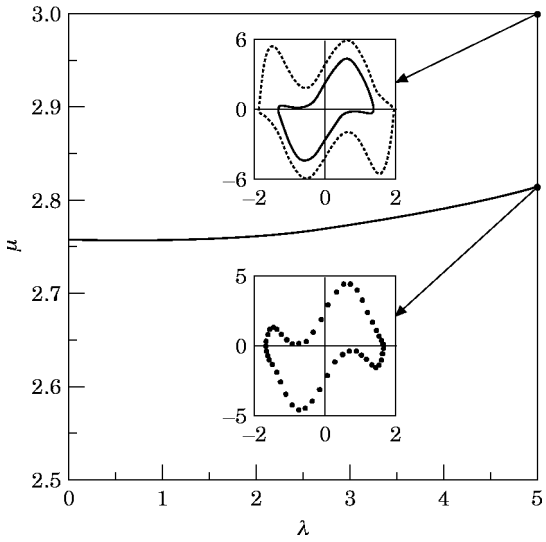

Figure 2. Limit cycle regions of equation (15) with phase portraits of the limit cycles for $\lambda = 5$ in case (1) $\mu = 2{\cdot}82146$ and case (2) $\mu = 3{\cdot}0$. Main diagram: (——), one limit cycle (semi-stable) $\mu^* = 2{\cdot}7573 + 0{\cdot}0012\,\lambda^{2{\cdot}413}$. Upper inset: Two limiting cycles; $\cdots$, unstable limit cycle (perturbation–incremental); (——), stable limit cycle (perturbation–incremental and numerical integration). Lower inset: $\cdots$, semi-stable limit cycle (perturbation–incremental).

The phase portrait of the semi-stable limit cycle of equation (15) for $\lambda = 5$ is also shown in Figure 2.

The stable and unstable limit cycles will now be further studied by following the same procedure as in [9]. Take as an example the particular value of $\mu = 3{\cdot}0$. The first step is to find the zero order approximation for the limit cycles. Two roots $a_0^{(1)}$ and $a_0^{(2)}$ are obtained from equation (21). Consequently, equation (19) has two solutions $\Phi_0^{(1)}(\varphi)$ and $\Phi_0^{(2)}(\varphi)$:

$$a_0^{(1)} = 1{\cdot}3207, \qquad \Phi_0^{(1)} = a_0^{(1)}[\tfrac{1}{2}(1 + \cos^2\varphi)]^{1/2}, \tag{24}$$

$$a_0^{(2)} = 2{\cdot}0032, \qquad \Phi_0^{(2)} = a_0^{(2)}\,[\tfrac{1}{2}(1 + \cos^2\varphi)]^{1/2}. \tag{25}$$

The second step is to apply the parameter incremental approach. $\lambda_0 = 0$, $\Delta\lambda = 0{\cdot}5$ and $M = 20$ are assigned to equations (14). After 10 successive increments of $\Delta\lambda$ starting from the zero order solutions (24) and (25) respectively, phase portraits of the results are shown also for $\lambda = 5$ in Figure 2. Checks using numerical integration schemes show that the results are very accurate.

4. EXAMPLE OF STABILITY BIFURCATION AND HETEROCLINIC BIFURCATION

As the second example, a generalized Rayleigh oscillator of the form

$$\ddot{x} + x - x^3 = \lambda(\mu - |\dot{x}|)\dot{x}, \qquad \lambda > 0, \tag{26}$$

is considered. For this example, $f(x, \dot{x}, \mu) = \mu - |\dot{x}|$, $g(x) = x - x^3$, hence $v(x) = \frac{1}{2}x^2 - \frac{1}{4}x^4$. Conditions (16–18) are satisfied. Equation (26) has fixed points at (0, 0), $(-1, 0)$ and $(1, 0)$. The origin (0, 0) is a focus and $(\pm 1, 0)$ are saddle points. For a fixed λ and an appropriate value of μ, there is a pair of heteroclinic orbits connecting the saddle points $(-1, 0)$ and $(1, 0)$ and surrounding the point (0, 0).

4.1. THE ZERO ORDER PERTURBATION SOLUTION

From equations (10) and (11b), one has

$$\Phi_0(\varphi) = [1 - \tfrac{1}{2} a_0^2 (1 + \cos^2 \varphi)]^{1/2} \tag{27}$$

and

$$\mu = \int_0^{2\pi} a_0 |\sin \varphi| \sin^2 \varphi \Phi_0^2(\varphi) \mathrm{d}\varphi \Big/ \int_0^{2\pi} \Phi_0 \sin^2 \varphi \, \mathrm{d}\varphi \overset{\text{def}}{=} \mu(a_0). \tag{28}$$

The limiting case at $a_0 = 1$ will correspond to $\mu = \bar{\mu}_0 = 2\sqrt{2}/5 \simeq 0{\cdot}56569$. Thus for $\lambda \approx 0$, the heteroclinic orbits can be described by the equations

$$x = \cos \varphi, \qquad \dot{x} = (-\sqrt{2}/2)|\sin \varphi| \sin \varphi. \tag{29}$$

Stability of the limit cycle is governed by equation (6). It becomes

$$\tilde{\gamma}_0 = \int_0^{2\pi} \frac{\mu(a_0) - 2a_0 |\sin \varphi| \Phi_0(\varphi)}{\Phi_0(\varphi)} \mathrm{d}\varphi. \tag{30}$$

The curves of both μ and $\tilde{\gamma}_0$ as functions of a_0 are plotted in Figure 3. The maximum value of μ from equation (28) is $\mu = \mu_0^*$ attained for $a_0 = a_0^*$, where

$$a_0^* \simeq 0{\cdot}96760, \qquad \mu_0^* \simeq 0{\cdot}56607. \tag{31}$$

These are the same values which satisfy equation (11c), i.e., to give $\tilde{\gamma}_0 = 0$. (the analytical proof of these results will be given in the Appendix). Thus the zero order approximation solution for the semi-stable limit cycle is given by

$$x = a_0^* \cos \varphi, \qquad \dot{x} = -a_0^* [1 - \tfrac{1}{2} a_0^* (1 + \cos^2 \varphi)]^{1/2} \sin \varphi. \tag{32}$$

Figure 3 shows that $\tilde{\gamma}_0 < 0$ for $a_0 < a_0^*$ and $\tilde{\gamma}_0 > 0$ for $a_0 > a_0^*$. General conclusions are that if $0 < \mu < \bar{\mu}_0$, equation (26) has one limit cycle. If $\bar{\mu}_0 < \mu < \mu_0^*$, equation (26) has two limit cycles with an unstable larger limit cycle and a stable smaller limit cycle. If $\mu > \mu_0^*$, equation (26) has no limit cycle. $\mu = \mu_0^*$ is the value of stability bifurcation where a

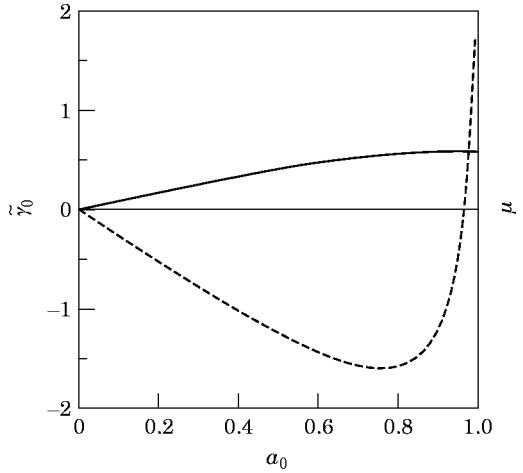

Figure 3. The parameter μ (——) and the characteristic exponent $\tilde{\gamma}_0$ (- - - -) versus amplitude a_0 of the limit cycle of equation (26) for the zero order perturbation solution.

TABLE 2

Values of μ^* and a at the semi-stable limit cycles of equation (26) *for various λ*

λ	μ^*	a
~ 0	0·56607	0·96760
1·0	0·55683	0·96832
2·0	0·53345	0·97363
3·0	0·50412	0·97966
4·0	0·47462	0·98496
5·0	0·44750	0·98120

$\mu^* \simeq 0{\cdot}566–0{\cdot}009\lambda^{1{\cdot}634}$

semistable limit cycle occurs. $\mu = \bar{\mu}_0$ is the value of heteroclinic bifurcation where a stable limit cycle and the heteroclinic orbits co-exist.

4.2. THE PARAMETER INCREMENTAL SOLUTION

Firstly, the results for stability bifurcation are extended to values of λ which are not necessarily small. $\lambda_0 = 0$ and $\Delta\lambda = 0{\cdot}5$ are assigned to equations (14). After 10 successive increments of $\Delta\lambda$ starting from solution (31), selected results are shown in Table 2.

Next, in order to determine the heteroclinic bifurcations, the additional requirement

$$a - 1 = 0 \tag{33}$$

governing the heteroclinic orbits should be imposed. Equation (9) will no longer apply and the complete set of equations consists of (3), (4), (5) and (33) only. Similar calculations have been performed in [10]. Some selected results are shown in Table 3.

The results of Table 2 and Table 3 are plotted in a (λ, μ) diagram in Figure 4. For $0 < \mu < \bar{\mu}$ (cf. region A in Figure 4), there is only one limit cycle and it is stable. At $\mu = \bar{\mu}$, there are one stable limit cycle and a pair of heteroclinic orbits. For $\bar{\mu} < \mu < \mu^*$ (region B), there are one stable limit cycle and one unstable limit cycle. At $\mu = \mu^*$, there is one semi-stable limit cycle. For $\mu > \mu^*$ (region C), no limit cycle exists.

Phase portraits of limit cycles and heteroclinic orbits for $\lambda = 1$ are shown in Figure 4(b) for four cases: $\mu = 0{\cdot}55$, 0·55653, 0·5567 and 0·55683.

5. EXAMPLE OF STABILITY BIFURCATION AND HOMOCLINIC BIFURCATION

As the last example, consider the generalized Rayleigh–Liénard oscillator of the form

$$\ddot{x} - x + x^3 = \lambda(\mu - x^2 - \dot{x}^2)\dot{x}, \qquad \lambda > 0. \tag{34}$$

TABLE 3

Values of $\bar{\mu}$ and a at the heteroclinic orbits of equation (26) *for various λ*

λ	$\bar{\mu}$	a
~ 0	0·56569	1·0
1·0	0·55653	1·0
2·0	0·53331	1·0
3·0	0·50407	1·0
4·0	0·47461	1·0
5·0	0·44750	1·0

$\bar{\mu} \simeq 0{\cdot}5657–0{\cdot}009\lambda^{1{\cdot}637}$

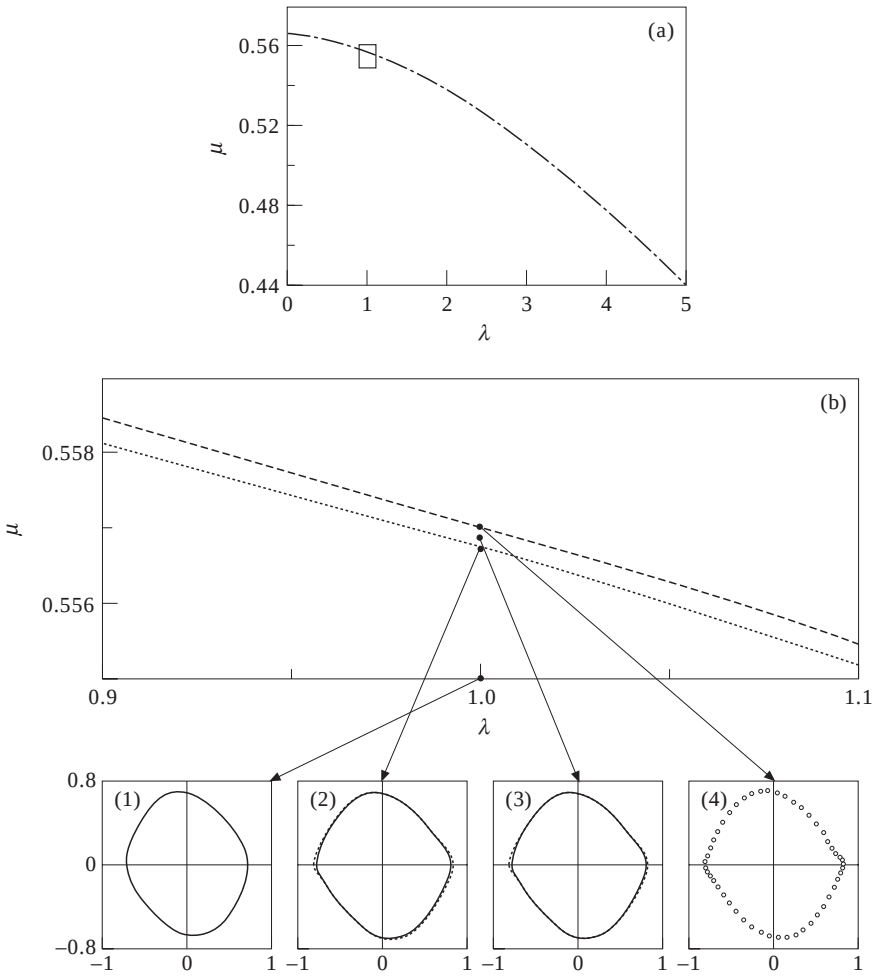

Figure 4. (a) λ, μ diagram of equation (26). (b) Expanded boxed region of Figure 4(a). Limit cycle regions of equation (26) with phase portraits of the limit cycles and heteroclinic orbits for $\lambda = 1$ in four cases. Initial expansion: - - - -, $\mu^* = 0{\cdot}566 - 0{\cdot}009\,\lambda^{1{\cdot}634}$; $\cdots$, $\bar{\mu} = 0{\cdot}5657 - 0{\cdot}009\,\lambda^{1{\cdot}637}$. Secondary expansions, μ values: (1) 0·55; (2) 0·55653; (3) 0·5567; (4) 0·55683.

Since $f(x, \dot{x}, \mu) = \mu - x^2 - \dot{x}^2$, $g(x) = -x + x^3$, hence $v(x) = -\frac{1}{2}x^2 + \frac{1}{4}x^4$. Equation (34) has fixed points at $(0, 0)$, $(-1, 0)$ and $(1, 0)$. The origin $(0, 0)$ is a saddle point and the points $(\pm 1, 0)$ are foci. For a fixed λ and an appropriate value of μ, there are two homoclinic orbits passing through the origin, one of which encircles the focus $(1, 0)$ and the other encircles the focus $(-1, 0)$. The discussion of the limit cycles will be separated into two parts.

5.1. Consider limit cycles enclosing all three fixed points. From equations (10) and (11b), one has

$$\Phi_0(\varphi) = [-1 + \tfrac{1}{2}a_0^2(1 + \cos^2\varphi)]^{1/2} \tag{35}$$

and

$$\mu = \int_0^{2\pi} (a_0^2\cos^2\varphi + a_0^2\,\Phi_0^2\sin^2\varphi)\Phi_0\sin^2\varphi\,\mathrm{d}\varphi \Big/ \int_0^{2\pi} \Phi_0\sin^2\varphi\,\mathrm{d}\varphi \overset{\text{def}}{=} \mu(a_0). \tag{36}$$

As Φ_0^2 must be non-negative for all φ, it follows $\min\Phi_0^2 = \Phi_0^2(\pi/2) = -1 + \frac{1}{2}a_0^2 \geq 0$, hence $a_0 \geq \sqrt{2}$. Letting $a_0 = \sqrt{2}$ and from equations (35) and (36), one obtains

$$\mu = \bar{\mu}_0 = \tfrac{8}{7}, \qquad \Phi_0(\varphi) = |\cos\varphi|. \tag{37}$$

For $\lambda \approx 0$, the pair of homoclinic orbits can be described by the equations

$$x = \sqrt{2}\cos\varphi, \qquad \dot{x} = -\sqrt{2}|\cos\varphi|\sin\varphi. \tag{38}$$

The curve generated by using equation (36) is shown in Figure 5. The minimum value of μ is $\mu_0^* \approx 1{\cdot}13266$ and it is attained for $a_0 = a_0^* \approx 1{\cdot}42193$.

Now consider the stability of the limit cycle. By substituting equations (35) and (36) into equation (11c), one obtains

$$a_0 = a_0^* \approx 1{\cdot}42193, \qquad \mu_0 = \mu_0^* \approx 1{\cdot}13266, \tag{39}$$

and the zero order approximation solution for the semi-stable limit cycle is then given by

$$x = a_0^*\cos\varphi, \qquad \dot{x} = -a_0^*[-1 + \tfrac{1}{2}a_0^{*2}(1 + \cos^2\varphi)]^{1/2}\sin\varphi. \tag{40}$$

For $\lambda \simeq 0$, equation (6) can be rewritten as

$$\tilde{\gamma}_0 = \int_0^{2\pi} \frac{\mu(a_0) - a_0^2\cos^2\varphi - 3a_0^2\Phi_0^2\sin^2\varphi}{\Phi_0}\,\mathrm{d}\varphi. \tag{41}$$

The curve generated by using equation (41) is also shown in Figure 5. The figure indicates that $\tilde{\gamma}_0 > 0$ for $a_0 < a_0^*$ and $\tilde{\gamma}_0 < 0$ for $a_0 > a_0^*$. The fact that the minimum values for equation (36) coincide with the zero values for equation (41) can be demonstrated analytically as given in the Appendix.

For small $\lambda > 0$, results are given in Figure 5. If $\mu_0^* < \mu < \bar{\mu}_0$, equation (34) has two limit cycles with an unstable smaller limit cycle and a stable larger limit cycle. If $\mu > \bar{\mu}_0$, equation (34) has one stable limit cycle. $\mu = \mu_0^*$ is the value of stability bifurcation and $\mu = \bar{\mu}_0$ is the value of homoclinic bifurcation.

By using the incremental procedure, values of stability bifurcations for different values of λ are obtained as shown in Table 4.

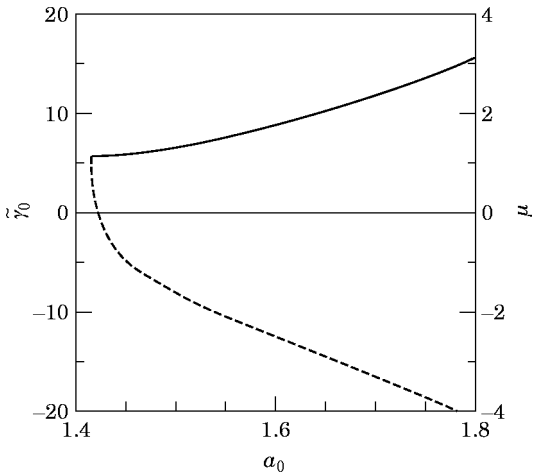

Figure 5. The parameter μ (——) and the characteristic exponent $\tilde{\gamma}_0$ (- - - -) versus amplitude a_0 of the limit cycle of equation (34) for the zero order perturbation solution.

TABLE 4

Values of μ^* and a at the semi-stable limit cycles of equation (34) *for various* λ

λ	μ^*	a
~ 0	1·13266	1·42193
1·0	1·10293	1·36694
2·0	1·06424	1·29585
3·0	1·04008	1·24712
4·0	1·02615	1·21416
5·0	1·01780	1·19062

$\mu^* \simeq 1{\cdot}13266 - 0{\cdot}0278\lambda^{0{\cdot}955}$

5.2. Consider limit cycles enclosing only one fixed point. As the trajectories of equation (34) are symmetrical with respect to the origin, phase portraits near the fixed points (1, 0) and $(-1, 0)$ are symmetrical. Therefore only the limit cycles at (1, 0) will be studied. Taking (1, 0) to be the new origin, equation (34) becomes

$$\ddot{x} + 2x + 3x^2 + x^3 = \lambda[\mu - (x+1)^2 - \dot{x}^2]\dot{x}. \tag{42}$$

Since $f(x, \dot{x}, \mu) = \mu - (x+1)^2 - \dot{x}^2$, $g(x) = 2x + 3x^2 + x^3$, hence $v(x) = x^2 + x^3 + \frac{1}{4}x^4$. Equations (10) and (11a) will give

$$b_0 = -1 + \sqrt{1 - a_0^2}, \qquad \Phi_0(\varphi) = [2 - \tfrac{5}{2}a_0^2 + 2a_0\sqrt{1 - a_0^2}\cos\varphi + \tfrac{1}{2}a_0^2\cos^2\varphi]^{1/2}. \tag{43}$$

As Φ_0^2 must be non-negative for all φ, it follows

$$0 < a_0 \leqslant \sqrt{2}/2. \tag{44}$$

When $a_0 = \sqrt{2}/2$, from equations (43) and (44), one obtains

$$b_0 = -1 + \sqrt{2}/2, \qquad \Phi_0(\varphi) = \tfrac{1}{2}[(\cos\varphi + 1)(\cos\varphi + 3)]^{1/2}. \tag{45}$$

Therefore, for $\lambda \approx 0$, the homoclinic orbit can be described by the equations

$$x = (\sqrt{2}/2)\cos\varphi - 1 + \sqrt{2}/2, \qquad \dot{x} = -(\sqrt{2}/4)[(\cos\varphi + 1)(\cos\varphi + 3)]^{1/2}\sin\varphi, \tag{46}$$

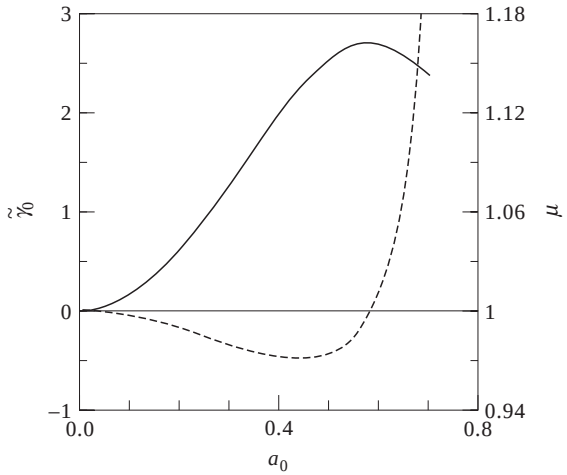

Figure 6. The parameter μ (——) and the characteristic exponent $\tilde{\gamma}_0$ (- - - -) versus amplitude a_0 of the limit cycle of equation (42) for the zero order perturbation solution.

TABLE 5

Values of $\tilde{\mu}^*$ with a and b at the semi-stable limit cycles of equation (42) *for various* λ

λ	$\tilde{\mu}^*$	a	b
~ 0	1·16070	0·57982	−0·18526
1·0	1·11887	0·51960	−0·17616
2·0	1·07145	0·42173	−0·14494
3·0	1·04458	0·33960	−0·10990
4·0	1·02964	0·27811	−0·08180
5·0	1·02084	0·23288	−0·06150

$\tilde{\mu}^* \simeq 1{\cdot}1607–0{\cdot}038\lambda^{0{\cdot}88}$

which passes through the other fixed point of equation (42) at $(-1, 0)$. From equations (11b) and (43), one has

$$\mu = \int_0^{2\pi} [(a_0 \cos\varphi + \sqrt{1-a_0^2})^2 + a_0^2\,\Phi_0^2 \sin^2\varphi]\Phi_0 \sin^2\varphi \,\mathrm{d}\varphi \Big/ \int_0^{2\pi} \Phi_0 \sin^2\varphi \,\mathrm{d}\varphi \overset{\text{def}}{=} \tilde{\mu}(a_0),$$

$$0 < a_0 < \sqrt{2}/2. \tag{47}$$

At $a_0 = \sqrt{2}/2$, $\tilde{\mu} = \bar{\mu}_0 = \frac{8}{7}$. The curve generated by using equation (47) is shown in Figure 6.

The maximum value $\tilde{\mu} = \tilde{\mu}_0^* \simeq 1{\cdot}16070$ is attained for $a_0 = \tilde{a}_0^* \simeq 0{\cdot}57982$.

Equation (6) can now be written as

$$\tilde{\gamma}_0 = \int_0^{2\pi} \frac{\tilde{\mu}(a_0) - (a_0\cos\varphi + \sqrt{1-a_0^2})^2 - 3a_0^2\,\Phi_0^2 \sin^2\varphi}{\Phi_0}\,\mathrm{d}\varphi. \tag{48}$$

The curve generated by using equation (48) is also shown in Figure 6. $\tilde{\gamma}_0 = 0$ will be located at $a_0 = \tilde{a}_0^*$ with $\tilde{\mu} = \tilde{\mu}_0^*$ (demonstration of this result is given in the Appendix). $\tilde{\gamma}_0 < 0$ for $a_0 < \tilde{a}_0^*$ and $\tilde{\gamma}_0 > 0$ for $a_0 > \tilde{a}_0^*$. The zero order approximation solution for the semi-stable limit cycle is then given by

$$x = \tilde{a}_0^* \cos\varphi - 1 + \sqrt{1-(\tilde{a}_0)^2}, \qquad \dot{x} = -\tilde{a}_0^*\,\Phi_0^*(\varphi)\sin\varphi, \tag{49}$$

where

$$\Phi_0^*(\varphi) = [2 - \tfrac{5}{2}(\tilde{a}_0^*)^2 + 2\tilde{a}_0^*\sqrt{1-(\tilde{a}_0^*)^2}\cos\varphi + \tfrac{1}{2}(\tilde{a}_0^*)^2\cos^2\varphi]^{1/2}.$$

The results of Figure 6 can be expressed as follows. If $1 < \mu < 8/7$, equation (42) has one stable limit cycle enclosing the origin, since $\tilde{\mu}(0) = 1$ and $\tilde{\mu}(\sqrt{2}/2) = \bar{\mu}_0 = \frac{8}{7}$. If $\bar{\mu}_0 < \mu < \tilde{\mu}_0^*$, equation (42) has two limit cycles enclosing the origin, with a stable smaller limit cycle

TABLE 6

Values of $\bar{\mu}$ with a and b at the homoclinic orbits of equation (42) *for various* λ

λ	$\bar{\mu}$	a	b
~ 0	1·14286	0·70711	−0·29290
1·0	1·10691	0·68176	−0·31824
2·0	1·06475	0·64752	−0·35248
3·0	1·04015	0·62348	−0·37652
4·0	1·02616	0·60706	−0·39294
5·0	1·01780	0·59631	−0·40469

$\bar{\mu} \simeq 1{\cdot}14286 - 0{\cdot}0325\lambda^{0{\cdot}903}$

and an unstable larger limit cycle. $\mu = \tilde{\mu}_0^*$ is the value of stability bifurcation and $\mu = \bar{\mu}_0$ is the value of homoclinic bifurcation.

For large values of λ, the results of the incremental procedure applied to stability bifurcations and homoclinic bifurcations are shown in Table 5 and Table 6 respectively.

Let one return now to equation (34) with the above conclusions as presented in Figure 7. There are seven distinct regions. For $1 < \mu < \mu^*$ (cf. region A in Figure 7), there are two

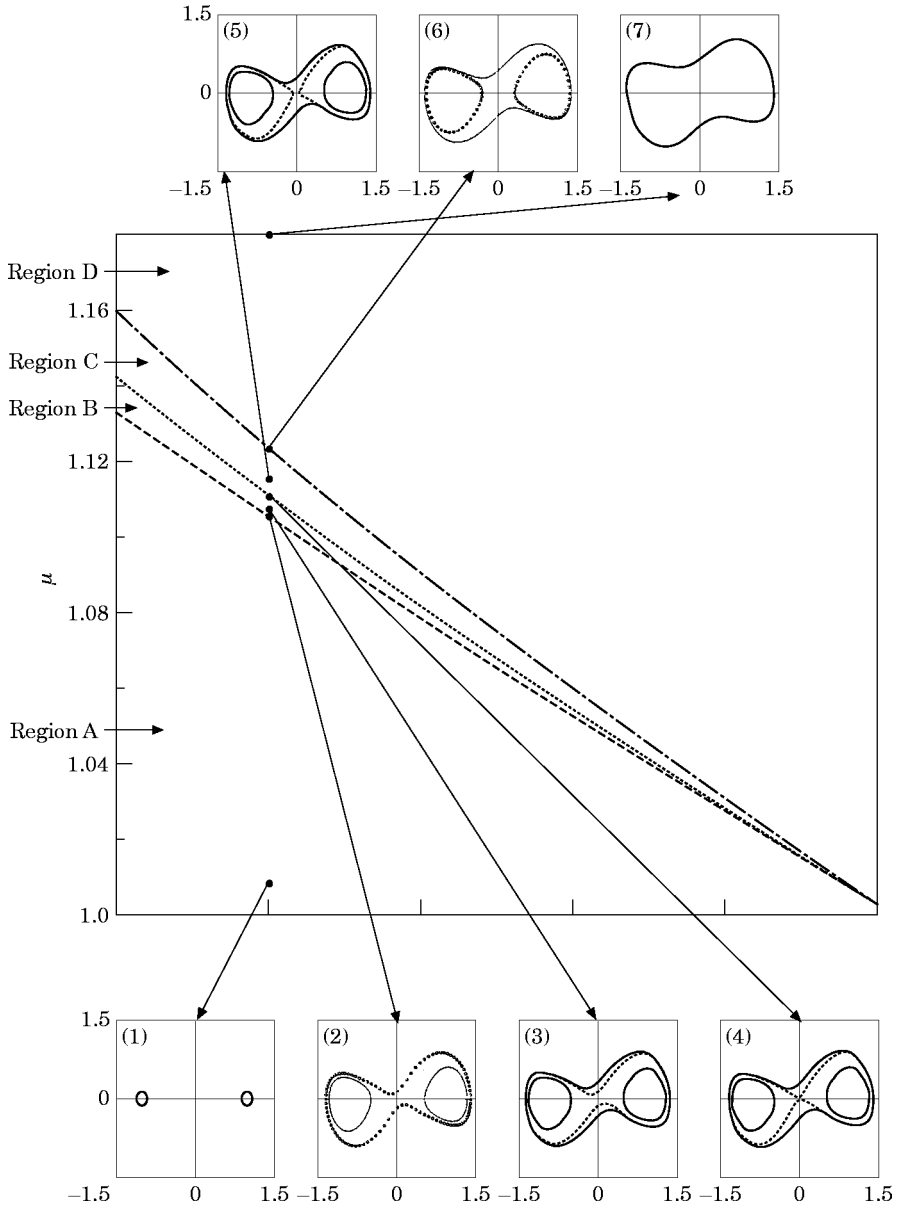

Figure 7. Limit cycle regions of equation (34) with phase portraits of the limit cycles and homoclinic orbits for $\lambda = 1$ in seven cases. Main figure: - - - - , $\mu^* = 1{\cdot}13266 - 0{\cdot}0278\lambda^{0{\cdot}995}$; $\cdots$, $\bar{\mu} = 1{\cdot}14286 - 0{\cdot}325$, $\lambda^{0{\cdot}903}$; $\cdot - \cdot -$, $\tilde{\mu}^* = 1{\cdot}1607 - 0{\cdot}038\lambda^{0{\cdot}88}$. μ values for phase portraits: (1) 1·01; (2) 1·10293; (3) 1·104; (4) 1·10691; (5) 1·109; (6) 1·11887; (7) 1·2.

limit cycles enclosing the fixed points $(\pm 1, 0)$ separately and they are stable (see phase portrait (1) in Figure 7). At $\mu = \mu^*$, apart from the two stable limit cycles enclosing the fixed points $(\pm 1, 0)$, there is one semi-stable limit cycle enclosing all three fixed points $(\pm 1, 0)$ and $(0, 0)$ (see phase portrait (2) in Figure 7). For $\mu^* < \mu < \bar{\mu}$ (region B), there are four limit cycles. One stable limit cycle and one unstable limit cycle both enclose all three fixed points, while the two stable limit cycles enclosing the individual fixed points $(\pm 1, 0)$ remain (see phase portrait (3) in Figure 7). At $\mu = \bar{\mu}$ there are a pair of homoclinic orbits, one stable limit cycle enclosing all three fixed points and two stable limit cycles enclosing the individual fixed points $(\pm 1, 0)$ separately (see phase portrait (4) in Figure 7). For $\bar{\mu} < \mu < \tilde{\mu}^*$ (region C), there are five limit cycles, one stable limit cycle enclosing all three fixed points, and pairs of stable and unstable limit cycles enclosing the individual fixed points $(\pm 1, 0)$ separately (see phase portrait (5) in Figure 7). At $\mu = \tilde{\mu}^*$ there are three limit cycles, one stable limit cycle enclosing all three fixed points and two semi-stable limit cycles enclosing the fixed points $(\pm 1, 0)$ separately (see phase portrait (6) in Figure 7). Finally for $\mu > \tilde{\mu}^*$ (region D), there is only one limit cycle enclosing all three fixed points and it is stable (see phase portrait (7) in Figure 7). The phase portraits (1–7) corresponding to these seven different cases are drawn for the particular values of $\mu = 1{\cdot}01$, $1{\cdot}10293$ (μ^*), $1{\cdot}104$, $1{\cdot}10691$ ($\bar{\mu}$), $1{\cdot}109$, $1{\cdot}11887$ ($\tilde{\mu}^*$) and $1{\cdot}2$.

6. CONCLUSION

The perturbation–incremental method has been used to study the stability bifurcations and homoclinic (heteroclinic) bifurcations of strongly non-linear oscillators. The limit cycles and the homoclinic (heteroclinic) orbits can be obtained with any arbitrary degree of accuracy. Results demonstrate that this procedure is an effective means in the study of global bifurcations.

REFERENCES

1. P. Holmes and D. Rand 1980 *International Journal of Non-Linear Mechanics* **15**, 449–458. Phase portraits and bifurcations of the non-linear oscillator: $\ddot{x} + (\alpha + \gamma x^2)\dot{x} + \beta x + \delta x^3 = 0$.
2. V. T. Coppola and R. H. Rand 1990 *Acta Mechanica* **81**, 125–142. Averaging using elliptic functions: approximation of limit cycles.
3. J. Garcia-Margallo and J. D. Bejarano 1990 *International Journal of Non-Linear Mechanics* **23**, 663–675. Stability of limit cycles and bifurcations of generalized van der Pol oscillators: $\ddot{x} + Ax - 2Bx^3 + \varepsilon(z_3 + z_2 x^2 + z_1 x^4)\dot{x} = 0$.
4. Z. Xu and J. B. Huang 1988 *Mechanics and Practice* **5**, 6–10. Practical analysis method for limit cycles of non-linear oscillators (in Chinese).
5. Z. Xu 1992 *Acta Mechanica Sinica* **8**, 279–288. Nonlinear time transformation method for strongly non-linear oscillation systems.
6. Z. Xu and Y. K. Cheung 1994 *Journal of Sound and Vibration* **174**, 563–576. Averaging method using generalized harmonic functions for strongly non-linear oscillators.
7. Z. Xu and Y. K. Cheung 1995 *Nonlinear Dynamics* **7**, 285–299. A non-linear scales method for strongly non-linear oscillators.
8. H. S. Y. Chan, K. W. Chung and Z. Xu 1995 *Journal of Sound and Vibration* **183**, 707–717. A perturbation-iterative method for determining limit cycles of strongly non-linear oscillators.
9. H. S. Y. Chan, K. W. Chung and Z. Xu 1996 *International Journal of Non-Linear Mechanics* **31**, 59–72. A perturbation-incremental method for strongly non-linear oscillators.
10. Z. Xu, H. S. Y. Chan and K. W. Chung 1996 *Nonlinear Dynamics* **11,** 213–233. Separatrics and limit cycles of strongly non-linear oscillators by the perturbation–incremental method.
11. Z. F. Zhang, T. R. Ding, W. Z. Huang and Z. X. Dong 1992 *Qualitative Theory of Differential Equations*. Providence, Rhode Island: AMS.

APPENDIX

The extreme value of μ occurs at the zero value of the characteristic exponent. Consider the special form of the function f given in the above examples:

$$f(x, \dot{x}, \mu) = \mu - h(x, \dot{x}).$$

From equation (15), μ can be expressed as

$$\mu = \int_0^{2\pi} h\Phi_0 \sin^2 \varphi \, \mathrm{d}\varphi \Big/ \int_0^{2\pi} \Phi_0 \sin^2 \varphi \, \mathrm{d}\varphi \tag{A1}$$

where it is known that $\Phi_0 = \Phi_0 (a_0, b_0, \varphi)$ and b_0 and a_0 are related by (11a). The authors intend to show that when μ attains an extreme value for $a = a^*$, (6) becomes

$$\tilde{\gamma}(a_0^*) = \int_0^{2\pi} (\mu - h + a_0^* \, \Phi_0 \sin \varphi h_{\dot{x}}') \frac{\mathrm{d}\varphi}{\Phi_0} = 0. \tag{A2}$$

Both sides of (10) are first partially differentiated to obtain, respectively,

$$a_0 \, \Phi_0 \frac{\partial}{\partial a_0} (a_0 \, \Phi_0 \sin^2 \varphi) = (1 + b_0')g(a_0 + b_0) - (\cos \varphi + b_0')g(a_0 \cos \varphi + b_0) \tag{A3}$$

where, from (11a),

$$b_0' = \mathrm{d}b_0/\mathrm{d}a_0 = [g(a_0 + b_0) + g_0 (-a_0 + b_0)]/[g(-a_0 + b_0) - g_0 (a_0 + b_0)]$$

and

$$\sin \varphi \, \partial\Phi_0 / \partial\varphi + \Phi_0 \cos \varphi = g(a_0 \cos \varphi + b_0)/a_0 \, \Phi_0. \tag{A4}$$

From (A3), one has

$$\int_0^{2\pi} \frac{\partial}{\partial a_0} (a_0 \, \Phi_0 \sin^2 \varphi) \, \mathrm{d}\varphi = \frac{(1 + b_0')g(a_0 + b_0)}{a_0} \int_0^{2\pi} \frac{\mathrm{d}\varphi}{\Phi_0} - \int_0^{2\pi} \Phi_0 \sin^2 \varphi \, \mathrm{d}\varphi. \tag{A5}$$

one lets

$$P(a_0) = \int_0^{2\pi} h\Phi_0 \sin^2 \varphi \, \mathrm{d}\varphi, \qquad P_1 (a_0) = a_0 \, P(a_0), \qquad Q(a_0) = \int_0^{2\pi} \Phi_0 \sin^2 \varphi \, \mathrm{d}\varphi, \tag{A6a–c}$$

and

$$Q_1 (a_0) = a_0 \, Q(a_0). \tag{A6d}$$

As μ attains an extreme value at $a = a^*$, it follows from (A1) and the condition $\mathrm{d}\mu/\mathrm{d}a_0 = 0$ that

$$\mu(a_0^*) = P(a_0^*)/Q(a_0^*) = P_1 (a_0^*)/Q_1 (a_0^*) = P_1' (a_0^*)/Q_1' (a_0^*). \tag{A7}$$

From (A5–7), one has

$$P_1' (a_0^*) = \mu(a_0^*) Q_1' (a_0^*) = K \int_0^{2\pi} \frac{\mu(a_0^*) \, \mathrm{d}\varphi}{\Phi_0} - P(a_0^*) \tag{A8}$$

where $K = (1 + b_0'^*)g(a_0^* + b_0^*)/a_0^*$ and $b_0'^* = \mathrm{d}b_0/\mathrm{d}a_0|_{a_0 = a^*}$. On the other hand, it follows from (A6a, b) that

$$P_1'(a_0) = \int_0^{2\pi} \frac{\partial}{\partial a_0}(a_0 h\Phi_0 \sin^2\varphi)\,\mathrm{d}\varphi = \int_0^{2\pi} a_0\,\Phi_0 \sin^2\varphi \frac{\partial h}{\partial a_0}\,\mathrm{d}\varphi + \int_0^{2\pi} h\frac{\partial}{\partial a_0}(a_0\,\Phi_0 \sin^2\varphi)\,\mathrm{d}\varphi. \tag{A9}$$

Using the partial differentiation identities

$$\frac{\partial h}{\partial a_0} = \frac{\partial h}{\partial x}\frac{\partial x}{\partial a_0} + \frac{\partial h}{\partial \dot{x}}\frac{\partial \dot{x}}{\partial a_0} = (\cos\varphi + b_0')h_x' + \left(\frac{(\cos\varphi + b_0')g(a_0\cos\varphi + b_0)}{a_0\,\Phi_0 \sin\varphi} - \frac{K}{\Phi_0 \sin\varphi}\right)h_{\dot{x}}',$$

$$\frac{\partial h}{\partial \varphi} = \frac{\partial h}{\partial x}\frac{\partial x}{\partial \varphi} + \frac{\partial h}{\partial \dot{x}}\frac{\partial \dot{x}}{\partial \varphi} = -a_0 \sin\varphi h_x' - \frac{g(a_0\cos\varphi + b_0)}{\Phi_0}h_{\dot{x}}',$$

and (A4, 9), one obtains

$$P_1'(a_0^*) = K\int_0^{2\pi} \frac{h d\varphi}{\Phi_0} - K\int_0^{2\pi} h_{\dot{x}}'\,a_0^* \sin\varphi\,\mathrm{d}\varphi - P(a_0^*). \tag{A10}$$

Comparing (A8) and (A10), one obtains

$$\int_0^{2\pi} \frac{\mu(a_0^*)}{\Phi_0}\,\mathrm{d}\varphi - \int_0^{2\pi} \frac{h\,\mathrm{d}\varphi}{\Phi_0} + \int_0^{2\pi} h_{\dot{x}}'\,a_0^* \sin\varphi\,\mathrm{d}\varphi = 0,$$

which implies (A2).